Superacid-Treated Silicon Surfaces: Extending the Limit of Carrier Lifetime for Photovoltaic Applications

Nicholas E. Grant, Tim Niewelt, Neil R. Wilson, Evangeline C. Wheeler-Jones, James Bullock, Mohammad Al-Amin, Martin C. Schubert, Andre C. van Veen, Ali Javey, and John D. Murphy

***Abstract*—Minimizing carrier recombination at interfaces is of extreme importance in the development of high-efficiency photovoltaic devices and for bulk material characterization. Here, we investigate a temporary room temperature superacid-based passivation scheme, which provides surface recombination velocities below 1 cm/s, thus placing our passivation scheme amongst state-of-the-art dielectric films. Application of the technique to high-quality float-zone silicon allows the currently accepted intrinsic carrier lifetime limit to be reached and calls its current parameterization into doubt for 1 Ω·cm n-type wafers. The passivation also enables lifetimes up to 65 ms to be measured in high-resistivity Czochralski silicon, which, to our knowledge, is the highest ever measured in Czochralski-grown material. The passivation strategies developed in this work will help diagnose bulk lifetime degradation under solar cell processing conditions and also help quantify the electronic quality of new passivation schemes.**

***Index Terms*—Lifetime, passivation, silicon, superacid (SA) treatment, surface recombination velocity.**

I. Introduction

EXCELLENT surface passivation of crystalline silicon is essential in the production of solar cells with efficiencies >25% and for accurate measurement of charge carrier diffusion lengths in high-quality substrates. Passivation of silicon surfaces had historically been achieved by high-temperature oxidation; however, current trends in photovoltaic (PV) research have since moved away from thermal oxidations due to:

1) the non-optimal refractive index of SiO_2,
2) the often negative impact of high-temperature processing on carrier diffusion lengths in Czochralski silicon (Cz-Si) and multicrystalline silicon (mc-Si) wafers [1]–[3], and
3) the excellent surface passivation offered by dielectric films which can be deposited by vacuum deposition systems at much lower temperatures ($\leq$400 °C).

Specifically, hydrogen-rich silicon nitride (SiN_x:H) [4], aluminum oxide (Al_2O_3) [5], and amorphous silicon (a-Si:H) [6] have all demonstrated surface recombination velocities (S) of $<$1 cm/s, with additional corona charging giving S as low as 0.1 cm/s in some cases [7]. It is, therefore, no surprise that a record efficiency of 26.6% [8] has been achieved by utilizing vacuum-deposited a-Si:H films for exceptional surface passivation, which in contrast to thermal oxidations, also retain very long carrier diffusion lengths during cell fabrication, owing to the low processing temperatures for this cell architecture ($<$300 °C).

In order to expand future avenues for silicon PV research, such as silicon/perovskite tandems [9] and materials characterization, alternative silicon surface passivation methods which do not involve complex vacuum deposition systems are required. Room temperature solution-based organic passivation of silicon is an exciting area for modern PV architectures. The most promising organic film developed thus far is poly(3,4 ethylenedioxythiophene):poly(styrenesulfonate) (PEDOT:PSS), which passivates the silicon surface and functions as a hole conducting layer [10]. Applications to the front textured surface of silicon solar cells have recently led to Yang *et al*. demonstrating open-circuit voltages (V_{oc}) of 634 mV and S of 100 cm/s [11] while Zhang *et al*. have reported the same V_{oc} of 634 mV applying the PEDOT:PSS passivating hole contact layer to the rear side of silicon-based solar cells [12]. In contrast, Schmidt *et al*. have demonstrated better electronic properties for rear-passivated PEDOT:PSS solar cells, where an emitter saturation current density (J_{oe}) of 80 fA/cm^2 and an implied open-circuit voltage (iV_{oc}) of 690 mV have been reported [13], [14]. This was further improved by Zielke *et al.*, who achieved J_{oe} of 46 fA/cm^2 by optimizing the silicon surface treatment prior to the deposition of PEDOT:PSS [15]. Omission of the conducting polymer PEDOT has led to

Manuscript received July 13, 2017; revised August 18, 2017; accepted September 6, 2017. This work was supported in part by the EPSRC SuperSilicon PV project (EP/M024911/1), in part by the EPSRC Global Challenges Research Fund (EP/P511079/1), in part by the EPSRC First Grant (EP/J01768X/2), and in part by the Royal Society (RG100076). *(Corresponding author: Nicholas E. Grant.)*

N. E. Grant, M. Al-Amin, A. C. van Veen, and J. D. Murphy are with the School of Engineering, University of Warwick, Coventry CV4 7AL, U.K. (e-mail: nicholas.e.grant@warwick.ac.uk; amin_srj@yahoo.com; andre.vanveen@warwick.ac.uk; john.d.murphy@warwick.ac.uk).

T. Niewelt and M. C. Schubert are with the Fraunhofer Institute for Solar Energy Systems ISE, Freiburg 79110, Germany (e-mail: tim.niewelt@ise.fraunhofer.de; martin.schubert@ise.fraunhofer.de).

N. R. Wilson is with the Department of Physics, University of Warwick, Coventry CV4 7AL, U.K. (e-mail: neil.wilson@warwick.ac.uk).

E. C. Wheeler-Jones is with the Department of Chemistry, University of Warwick, Coventry CV4 7AL, U.K. (e-mail: e.wheeler-jones@warwick.ac.uk).

J. Bullock and A. Javey are with the Department of Electrical Engineering and Computer Sciences, University of California, Berkeley, CA 94720 USA (e-mail: james.bullock@berkeley.edu; ajavey@berkeley.edu).

Color versions of one or more of the figures in this paper are available online at http://ieeexplore.ieee.org.

Digital Object Identifier 10.1109/JPHOTOV.2017.2751511

Chen *et al*. demonstrating a high level of surface passivation by depositing just PSS, which after a short heat-treatment at 130 °C for 10 min yields $iV_{\rm oc}$ of 700–710 mV and *S* of 4–5 cm/s on n- and p-type silicon [16]. While PEDOT: PSS and PSS films are promising approaches to contacting or passivating silicon, they do exhibit severe degradation under ambient conditions, and thus require capping films in order to inhibit degradation [13].

Recently, Bullock *et al*. have developed an organic passivation method in which silicon wafers are briefly dipped in a nonaqueous bis(trifluoromethane)sulfonimide (TFSI) superacid (SA) solution. By this procedure, an upper limit *S* of 3 and 13 cm/s on n- and p-type silicon are achieved, respectively [17]. From all these recent studies, it is evident that organic films can provide exceptional silicon surface passivation at very low temperatures ($<$200 °C), which could open up other opportunities for new and innovative low-temperature gettering and hydrogenation techniques to improve low-quality silicon for their inclusion as the base material in highly efficient solar cells [18]–[21]. However, the level of surface passivation demonstrated until now (>1 cm/s) is not good enough to compete with state-of-the-art dielectric films.

In this work, we develop an organic passivation procedure for materials characterization and potential future PV device applications. The procedure incorporates the previously described SA method of Bullock *et al*. [17] and enables us to reduce *S* below 1 cm/s. We demonstrate the surface passivation achieved by immersion in a TFSI-containing solution is sensitive to the pre-treatment cleaning/etching procedures and also to humidity, yet can be sufficiently stable for short term ($\sim$3 h) photoconductance (PC) and photoluminescence (PL) imaging measurements. Through etch-back experiments (etching silicon and re-passivation of the surfaces), we demonstrate $S < 1$ cm/s can be achieved on silicon with a phosphorus/boron doping concentration of $<5.0 \times 10^{15}$ cm^{-3}, and provide a parameterization for *S* when silicon wafers are passivated by the SA treatment. The quality of our surface passivation enables the measurement of lifetimes up to, and possibly beyond, the intrinsic lifetime limit, casting doubt over its currently accepted parameterization [5]. Finally, we demonstrate the capabilities of the passivation scheme by diagnosing bulk lifetime degradation under standard solar cell processing conditions.

II. Experimental Details

All silicon wafers used had a crystal orientation of (100) and a wafer diameter of 100 mm unless otherwise specified. Samples studied were quarter wafers. Table I summarizes the various silicon materials used in this work.

TABLE I
Material Specifications

Growth Method	Resistivity (Ω·cm)	Type (n/p)	Thickness *W* (μm)	Initial Surface Condition
Section III-A				
FZ	2	n	360	Mechanical polish
Section III-B				
FZ$^{\chi}$	75	n	320	Mechanical polish
Cz†	1270	n	750	Mechanical polish
Section III-C–E				
FZ	1	n	200	Chemical polish
FZ	10	n	200	Chemical polish
FZ	1	p	200	Chemical polish
FZ	10	p	240	Chemical polish
FZ	5	n	750	Mechanical polish

The oxygen concentration in the Cz substrate was $[O_i] = 8 \times 10^{17}$ cm^{-3} according to the DIN50438/I (1995) calibration standard.
$^{\chi}$ A 5 cm × 5 cm sample was cleaved from a 150 mm diameter wafer.
† A 5 cm × 5 cm sample was cleaved from a 200 mm diameter wafer.

A. Passivation Solution Preparation

In order to minimize moisture contamination during solution preparation, chemicals were measured and mixed in a glovebox purged with nitrogen (N_2). To prepare the solution, 100 mg of bis(trifluoromethane)sulfonimide (Sigma-Aldrich, 95%) was measured out and then dissolved in 50 ml of anhydrous 1, 2-dichloroethane (Sigma-Aldrich, 99.8%), in accordance with the optimum recipe described in [17]. Once prepared, the solution was stored in a glass container with an air-tight cap. We have found the solution can be used successfully multiple times, but when the solution becomes cloudy (evidence of too much moisture), a new solution must be prepared.

B. Wet Chemical Pre-treatment

Performing the optimum chemical pre-treatment of the silicon surface is a vital part of the passivation process. The water used must be deionized (DI) water of very high purity. In our experiments, the DI water had a measured resistivity of 18 MΩ and an organic impurity level of $<$50 ppb.

Unless otherwise specified, our optimized process is that wafers were initially dipped in 1% HF to remove the native oxide, subjected to standard clean 2 (SC 2) consisting of H_2O, H_2O_2 (30%), HCl (37%) (5:1:1) for 5 min at $\sim$75 °C [22], dipped in 1% HF to remove the chemical oxide formed and then etched in 25% tetramethylammonium hydroxide (TMAH) for 10 min at $\sim$80 °C. Following the TMAH etch, the samples were dipped in 1% HF and subsequently cleaned in the SC 2 solution for 10 min at $\sim$75 °C. To complete the surface pre-treatment, the silicon samples were immersed (individually) in 2% HF for 5 s and pulled dry from the HF solution. At this point, the samples were not rinsed in DI water.

C. Surface Passivation Procedure

Immediately following the surface pre-treatment, the silicon samples were placed in a plastic petri-dish and were transferred to a glovebox. The glovebox was purged with N_2 until a relative humidity of $<$25% was achieved. The prepared SA solution (see Section II-A) was poured into a glass beaker and then a silicon sample was immersed in the solution for $\sim$60 s. The sample was then removed from the solution and then dried in the glovebox under N_2 ambient. During this time, the solvent evaporates very quickly from the surface and becomes dry within $\sim$30 s. At

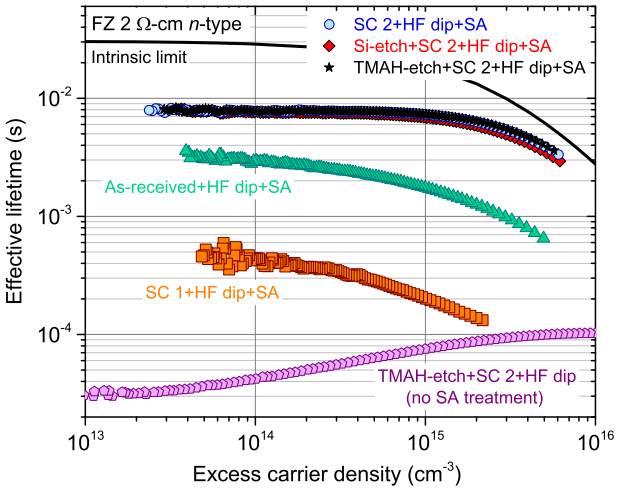

Fig. 1. Effective lifetime versus excess carrier density for mirror polished FZ 2 Ω·cm n-type silicon which has undergone different wet chemical surface treatments followed by an SA treatment. The pre-treatments were SC 1 + HF dip + SA (orange squares), as-received + HF dip + SA (green triangles), SC 2 + HF dip + SA (blue circles), Si-etch (HF:HNO_3) + SC 2 + HF dip + SA (red diamonds), TMAH-etch + SC 2 + HF dip + SA (black stars), and TMAH-etch + SC 2 + HF dip with no SA treatment (purple pentagons).

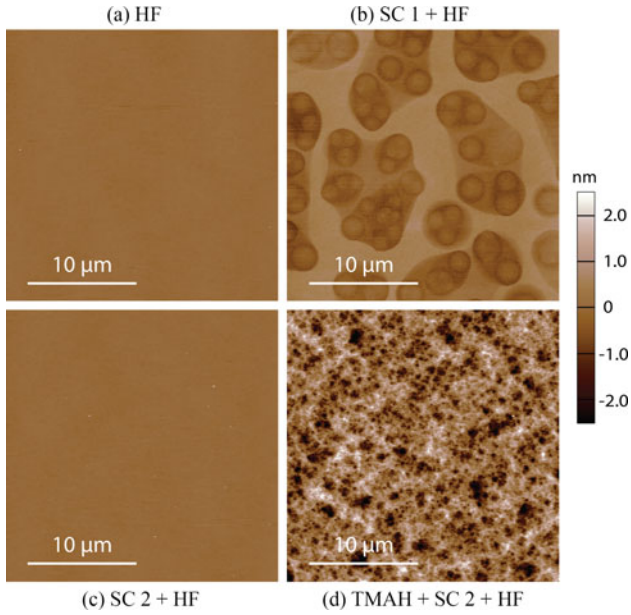

Fig. 2. Representative 25 μm × 25 μm AFM images of initially mirror polished FZ 2 Ω·cm n-type silicon after (a) a 2% HF dip, (b) SC 1 + 2% HF dip, (c) SC 2 + 2% HF dip, and (d) 25% TMAH etch + SC 2 + 2% HF dip. All images are on a 5 nm roughness scale. The silicon samples measured here have not been SA treated.

this point, the passivated sample can be removed from the glovebox and measured by the techniques presented in Section II-D.

For comparison purposes, samples featuring Al_2O_3 passivation (10 nm per side) were deposited by atomic layer deposition (ALD) at 180 °C. To activate this surface passivation, samples were annealed in forming gas (5% H_2 in 95% N_2) at 425 °C for 25 min.

D. Measurement Procedure

Minority carrier lifetime measurements were performed using a Sinton WCT-120 PC lifetime tester under transient PC mode [23] while calibrated lifetime maps were obtained by a BT Imaging LIS-L1 PL imaging system [24]. PL images were acquired with excitation by LEDs with a wavelength of 650 nm. A ±5% uncertainty in the lifetime measurements was assumed for each dataset [25].

In some samples, the silicon surface microtopography was measured using an atomic force microscope (AFM) and data were acquired in the ac mode (tapping mode) on an Asylum Research MFP3D-SA system.

The resistivity of the silicon wafers was measured by a four-point probe using a Jandel RM3000 model. The error in the measured resistivity is ±0.3%. The thickness of the silicon samples was determined by measuring their weight using a precision balance (KERN EMB 100-3), after correcting for surface area and the density of silicon (2.329 g/cm^3). Here, we assume the sample thickness is plane-parallel due to the isotropic etching nature of TMAH on (100) oriented silicon surfaces.

III. Results and Discussion

A. Wet Chemical Pre-treatment

Fig. 1 plots the injection-dependent effective lifetime (τ_{eff}) of mirror polished FZ 2 Ω·cm n-type silicon after trialed wet chemical pre-treatments and a subsequent SA passivation treatment (see Section II). The figure demonstrates that surface passivation adequate for many purposes ($\tau_{\text{eff}} > 1$ ms), can be achieved if "new" silicon wafers are taken from the manufacturer's box and are simply dipped in a 2% HF solution (until hydrophobic) followed by an SA treatment. In this case, however, the passivation quality will depend on the initial surface condition of the silicon wafers obtained from the manufacturer. That is, mechanical/chemical polished wafers may give different results to those which have been damage etched. Furthermore, the level of cleanliness on as-received wafers could be variable and thus lead to inconsistent results and lower passivation levels.

When the silicon wafers were subjected to an SC 1 clean (also known as RCA 1), consisting of H_2O, H_2O_2 (30%), NH_4OH (30%) (5:1:1) at ∼75 °C [22], followed by a 2% HF dip and SA treatment, a significant decrease in the measured lifetime (< 1 ms) was observed as shown in Fig. 1. The cause for this significant reduction in effective lifetime is not well understood but was observed consistently. It is widely believed that microroughening of the silicon surface during SC 1 cleaning can occur due to the etching behavior of ammonium hydroxide [26]–[28]. In this case, oxidation of the silicon surface occurs by reactions with H_2O^- and etching of the silicon dioxide film/silicon occurs by reactions with OH^- (originating from the breakdown of NH_4^+). Under these conditions, the silicon surface is continually being etched by either 1) continual etching and regrowth of the oxide film or 2) by direct reactions with OH^-, which result in much rougher silicon surfaces compared to 1) [26]. The AFM roughness maps presented later (see Fig. 2) demonstrate that etching of the surface during SC 1 cleaning does occur; however, this may not be the primary reason for the large reduction in lifetime shown in Fig. 1 as discussed later.

As an alternative to SC 1 cleaning, we also investigated immersing the silicon wafers in SC 2 (see Section II-B) followed

by a 2% HF dip and SA treatment. Contrary to SC 1, SC 2 provides a favorable surface pre-conditioning for SA-treated silicon which results in very high effective lifetimes of $\sim$8 ms (at $\Delta p < 10^{15}$ cm^{-3}), which is an order of magnitude higher than achieved with SC 1. Moreover, SC 2 solutions do not etch the silicon surface or any oxides that form during the cleaning step [29], and this will be demonstrated by our AFM images shown in Fig. 2. Therefore, we attribute this difference in surface chemistry between SC 1 and SC 2 cleans to the level of surface passivation achieved when passivating the silicon surfaces using the SA treatment. While SC 2 cleaning does result in much higher lifetimes, we postulate this wet chemical pre-treatment will still depend on the surface condition of the wafers, and therefore it is likely this pre-treatment will result in unreliable surface passivation if, for example, silicon wafers were "as-cut" or previously passivated with a dielectric film.

In order to minimize surface passivation inconsistencies due to differences in as-received silicon surfaces, we have examined etching silicon wafers in either a HF (50%), HNO_3 (69%) (1:10) mixture for 1 min or 25% TMAH for 10 min at $\sim$75 °C followed by SC 2 cleaning, a final 2% HF dip, and SA treatment. Fig. 1 demonstrates that both etching solutions provide an optimal surface condition for SA-treated silicon, achieving near identical lifetimes of $\sim$8 ms (at $\Delta p < 10^{15}$ cm^{-3}). Without the final SA treatment, however, the measured lifetime is very low ($< 100\,\mu$s) as also shown in Fig. 1, thereby demonstrating the necessity of the SA treatment, irrespective of the various wet chemical pre-treatments. While the lifetime of a TMAH-etch + SC 2 + HF dip + SA treatment is similar to that achieved by a single SC 2 + HF dip + SA treatment, the etching process will in most cases achieve the same surface condition after every etch, and therefore should be independent of the surface condition prior to etching (polished versus as-cut). In most practical cases, silicon wafers are commonly etched to remove saw damage, diffusions, or to smoothen the silicon surface prior to surface passivation, and therefore the results of Fig. 1 indicate etching does not degrade the performance of SA-treated silicon but rather improves it (excluding cases where the wafers are already mirror polished) provided the correct sequence of wet chemical cleaning is performed. We note that without a subsequent SC 2 clean and HF dip following the etching process, non-optimal passivation will result (not shown).

To elucidate the surface passivation dependence of SA-treated silicon on pre-treatment chemical processes, we have performed AFM topographical imaging of the surface condition following each of the treatments listed in Fig. 1; however, in this case, no subsequent SA treatment was performed. Fig. 2(a) and (c) show AFM images of very smooth silicon samples that underwent a single 2% HF dip and an SC 2 clean respectively, which despite the different chemical processes exhibit near identical surface conditions as identified by the roughness average (R_a) values presented in Table II. It is noted that this is not reflected in the lifetimes shown in Fig. 1, whereby an SC 2 cleaned surface attains a much higher lifetime than an HF dipped surface following an SA treatment. This difference in lifetime could be explained by some level of surface contamination on the HF dipped surface, thereby highlighting the necessity of a chemical clean/etch to remove surface impurities. The exceptionally smooth surface maintained following an SC 2 clean is consistent with the growth of a thin oxide film which is not etched/attacked while immersed in the SC 2 solution as described in [29].

TABLE II
AFM ROUGHNESS AVERAGE (R_a) VALUES

Wet chemical treatment	Average roughness R_a (nm)
HF	0.07 ± 0.02
SC 1 + HF	0.36 ± 0.05
SC 2 + HF	0.07 ± 0.01
TMAH + SC 2 + HF	0.88 ± 0.02

The scan size was 25 μm $\times$ 25 μm and scans were performed in multiple locations on the sample surface.

In contrast, Fig. 2(b) (SC 1) and (d) (TMAH etched) show markedly different features that result in significantly different surface passivation (after SA treatment) levels as shown in Fig. 1. Fig. 2(b) shows that SC 1 cleaning results in a surface condition featuring large, up to 1 nm in depth, symmetrical etch pits which are uniformly distributed across the silicon surface. In this case, it is evident that SC 1 cleaning solutions do etch the silicon surface, which is consistent with [26]. Notably, in-between the large etch pits, the silicon surface is very smooth and therefore simply quoting its roughness value ($R_a \approx 0.36 \pm 0.05$ nm) for this surface is not an accurate description of the surface condition. In contrast, a TMAH etched surface shows [see Fig. 2(d)] a much rougher surface ($R_a \approx 0.88 \pm 0.02$ nm) compared to an SC 1 prepared sample; however, it exhibits a much higher level of surface passivation as shown in Fig. 1, thereby indicating the SA treatment is to some extent not dependent on the smoothness of the silicon surface. Because of this, we do not attribute the etch pits in Fig. 2(b) (SC 1) as the primary contributor to the very low level of surface passivation attained on this surface.

It is instructive to note that while the AFM images of SC 2 [see Fig. 2(c)] and TMAH [see Fig. 2(d)] treated surfaces are markedly different, their level of surface passivation (after SA treatment) is near identical (see Fig. 1). However, given that both surfaces have undergone an SC 2 and 2% HF dip as the final treatment, we attribute these last processes as the key factor in the achievement of exceptional passivation. Similarly, if an SC 1 treated surface (which degrades the level of subsequent passivation) is followed by an SC 2 clean, a large recovery in surface passivation is obtained (not shown), thereby further signifying the importance of the SC 2 process prior to the SA treatment. Considering the purity of the chemicals and DI water used during our experiments, we do not attribute removal of metal impurities as the main contributor to the enhanced passivation of the SC 2 process over SC 1. Furthermore, SC 1 can also remove metal impurities [22].

In terms of the passivating species following the SA treatment, Bullock *et al.* have demonstrated through Fourier transform infrared spectroscopy and X-ray photoelectrons spectroscopy, that "TFSI-like" species are detectable on the silicon surface following the treatment [17]. At this time, however, it is difficult to ascertain whether TFSI is directly involved in passivating the

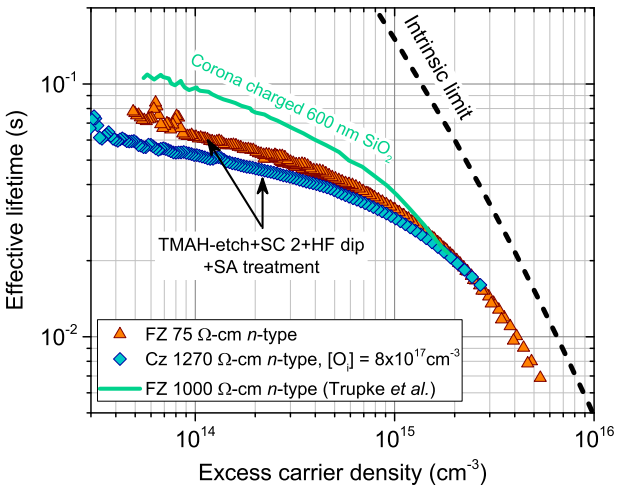

Fig. 3. Injection-dependent lifetime curves of high-quality silicon materials. Our data are with SA-treated wafers after a wet chemical pre-treatment in 25% TMAH, SC 2 clean, and 2% HF dip, and are for 320 μm thick FZ 75 Ω·cm n-type silicon (orange triangles) and 750 μm thick Cz 1270 Ω·cm n-type silicon (blue diamonds). For comparison, data for thermally oxidized (600 nm) and corona charged 525 μm thick FZ 1000 Ω·cm n-type silicon by Trupke *et al.* [30] are shown (green line). As far as we are aware, this is the highest lifetime (at low Δp) ever reported for silicon. The dashed black curve represents the intrinsic parameterization by Richter *et al.* [5].

silicon surface, or whether the TFSI undergoes a reaction with the solvent, splitting the TFSI into smaller species which can then readily passivate the silicon surface. In this regard, more work is required before a detailed passivation mechanism can be proposed.

In summary, from the results of Figs. 1 and 2, we conclude that to achieve a reliably high level of surface passivation using an SA solution, silicon wafers should undergo a chemical etch in either HF:HNO_3 or 25% TMAH at $\sim$75 °C followed by an SC 2 clean and HF dip.

B. Superacid-Treated Silicon for Extremely Long Lifetime Measurements

To demonstrate the high level of surface passivation attained by the SA treatment following the optimal wet chemical pre-treatment (TMAH etch + SC 2 + 2% HF dip), Fig. 3 plots the effective lifetime of three different high-resistivity Cz and FZ silicon wafers passivated using SA.

From Fig. 3, it is evident that a very high level of surface passivation is attained by SA-treated high-resistivity FZ-Si and Cz-Si wafers. Maximum respective lifetimes of $\sim$75 ms (orange triangles) and $\sim$65 ms (blue diamonds) are measured at low Δp, which correspond to S (after correcting for intrinsic recombination using Richter *et al.*'s parameterization [5]) of 0.2 and 0.6 cm/s, respectively. Such high lifetimes are very rarely reported, and to the best of our knowledge, we are reporting the highest lifetime ever measured in Cz-Si. In FZ-Si, however, we are aware that Trupke *et al*. have measured lifetimes exceeding 100 ms (130 ms max) [30], and their data are also plotted in Fig. 3. To measure such high lifetimes, Trupke *et al.* used a passivation scheme based on a corona charged 600 nm thick thermal oxide layer, which in comparison to the SA treatment is far more difficult to produce and exposes the wafers to a high thermal budget. Interestingly, if the maximum lifetime of 130 ms is converted to a surface recombination value, we estimate S to be 0.2 cm/s (after correcting for intrinsic recombination [5]), which is identical to our value for S in FZ-Si, thereby implying the difference in lifetime between the FZ wafers is purely background doping related, i.e., intrinsic recombination due to the difference in doping concentrations. Therefore, our lifetime in FZ-Si of 75 ms at low Δp, and a corresponding diffusion length of $\sim$1 cm (30$\times$ larger than the wafer thickness), is amongst the highest ever reported for $<1000\,\Omega$·cm silicon, and demonstrates the quality of the SA passivation scheme, equivalent to *in situ* liquid passivation schemes using HF-based solutions for measuring high lifetime materials [31]–[33].

C. Quantifying Surface Recombination of Superacid-Treated Silicon

To evaluate the surface recombination velocity achieved by the SA treatment, silicon wafer quarters underwent etch-back and re-passivation experiments, in which a planar chemical etch is used to thin the same silicon wafer between measurements. In this procedure, the effective lifetime ($\tau_{\rm eff}$) will decrease proportionally with the thickness W of the silicon wafer according to [34]

$$\frac{1}{\tau_{\rm eff}} = \frac{1}{\tau_{\rm bulk}} + \frac{2S}{W}. \tag{1}$$

Therefore, plotting $1/\tau_{\rm eff}$ against $1/W$ for each measurement yields a straight line where the intercept is $1/\tau_{\rm bulk}$ and the slope is $2S$, where $\tau_{\rm bulk}$ corresponds to the bulk lifetime.

Prior to the etch-back experiments, 1, 10 Ω·cm n- and p-type FZ wafers (100 mm diameter) were subjected to a phosphorus diffusion in a quartz tube furnace at 840 °C for 60 min. After removal of the phosphosilicate glass in buffered HF and subsequent SC cleaning, the wafers were thermally oxidized in oxygen (with background dichloroethylene) for 60 min at 1050 °C. The oxidation annihilates grown-in defects [35], [36] while the phosphorus diffusion getters impurities and prevents external contamination during the high-temperature oxidation. Following the high-temperature processing, the SiO_2 film and phosphorus diffused region were chemically etched away. One set of wafers was then subjected to ALD Al_2O_3 passivation (10 nm on each side) as a reference, and wafers from the other set were quartered for etch-back experiments using SA as the passivation scheme. Prior to the SA treatment (during the etch-back experiment), the silicon samples were subjected to a 200 °C anneal for 30 min in order to inhibit bulk degradation [37]. Following the anneal, the samples were etched in 25% TMAH for 20–30 min at $\sim$80 °C followed by SC 2 cleaning, 2% HF dip, and SA treatment. This process was repeated multiple times on the same quarters in order to gather the dataset required to extract $\tau_{\rm bulk}$ and S using (1). We note, this method is experimentally challenging, and accurate measurements of $\tau_{\rm bulk}$ and S are difficult to achieve if the measured lifetime curves feature noise. In our work, extracted $\tau_{\rm bulk}$ and S values at $\Delta n < 5.0 \times 10^{14}$ cm^{-3}

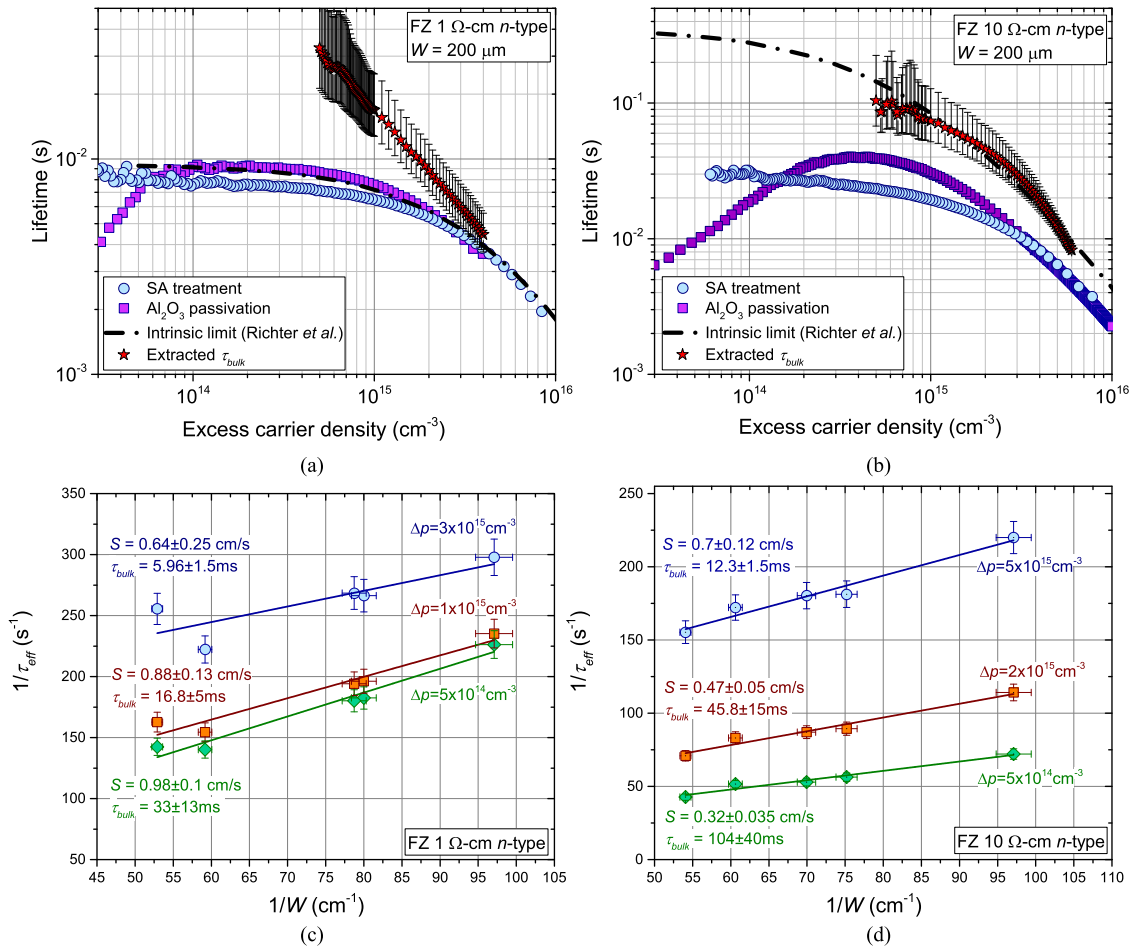

Fig. 4. Graphs (a) and (b) show the respective injection-dependent lifetime of 1 Ω and 10 Ω·cm n-type FZ-Si passivated with superacid (blue circles) and Al_2O_3 (purple squares). The red stars represent the extrapolated bulk lifetime from etch-back experiments using the SA treatment and the dashed black line corresponds to the intrinsic limit [5]. In accordance with Eq. (1), graphs (c) and (d) show reciprocal effective lifetime against the reciprocal wafer thickness for SA-treated FZ 1 and 10 Ω·cm n-type silicon at different injection levels.

(in most cases) could not be accurately measured due to noise in the measured lifetime curves.

1) n-type Silicon: Fig. 4(a) and (b) show the injection-dependent effective lifetime of Al_2O_3 (purple squares) and SA (blue circles) treated n-type silicon. The figures demonstrate that both schemes exhibit similar passivation levels; however, the slight benefit of Al_2O_3 passivation over the SA treatment is diminished when considering the injection dependence of each passivation scheme. For Al_2O_3 passivation, the films are well known to possess a large negative charge [38], which on n-type silicon depletes the silicon surface of majority carriers, thereby increasing surface recombination in mid to low injection as evident in both Fig. 4(a) and (b). In contrast, SA-treated n-type silicon does not show such injection dependence, which demonstrates its advantage over Al_2O_3 for bulk defect examination/analysis, irrespective of the slightly lower passivation quality under these conditions. Furthermore, the lack of injection dependence indicates the passivating film does not contain a significant level of negative charge, which is consistent with the initial SA report [17]. Therefore, the slightly lower lifetimes (compared to Al_2O_3 passivation) at moderate injection levels for SA-treated n-type silicon is likely due to a low density of charge at the surfaces.

Fig. 4(c) and (d) plot the reciprocal effective lifetime against the reciprocal wafer thickness for SA-treated FZ 1 and 10 Ω·cm n-type silicon at different injection levels. After applying linear regressions to fit the experimental data, $\tau_{\rm bulk}$ and S were determined with reasonable uncertainty. For the 1 Ω·cm n-type sample [see Fig. 4(a)], we measure an astonishingly high bulk lifetime of 16.8 ± 5 ms and a very low S of 0.88 ± 0.13 cm/s (at $\Delta p = 10^{15}$ cm^{-3}). For the 10 Ω·cm n-type sample [see Fig. 4(b)], we measure a bulk lifetime of 74 ± 25 ms and a very low S of 0.36 ± 0.04 cm/s (at $\Delta p = 10^{15}$ cm^{-3}). Furthermore, Fig. 4(c) and (d) demonstrate the exceptional consistency of the SA treatment, which permits the accurate extraction of both $\tau_{\rm bulk}$ and S.

Turning back to the extracted bulk lifetime, Fig. 4(a) plots $\tau_{\rm bulk}$ which is considerably higher than the modeled intrinsic limit for the same doping concentration [5]. In contrast, the effective lifetime of the Al_2O_3 passivated sample also exceeds the intrinsic limit, which has also been observed by other groups [39], [40], thereby implying the true bulk lifetime is indeed

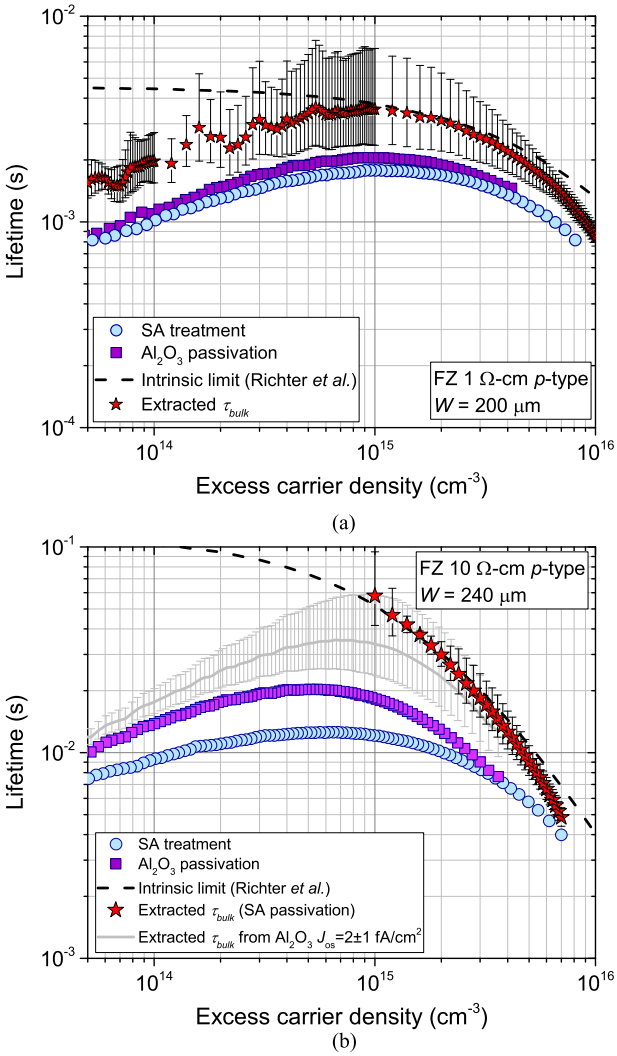

Fig. 5. Injection-dependent lifetime of FZ 1 Ω·cm [graph (a)] and 10 Ω·cm [graph (b)] p-type silicon passivated with superacid (blue circles) and Al_2O_3 (purple squares). The red stars in each figure represent the extrapolated bulk lifetime from etch-back experiments using the SA treatment and the dashed black line corresponds to the intrinsic limit [5].

higher than that given by the current parameterization. In light of this discovery, a re-evaluation of the intrinsic recombination (radiative and Auger) should be performed. Unlike the previous versions of Richter *et al*. [5], Kerr and Cuevas [41], and Schmidt *et al*. [42], it is recommended that this should include an in-depth analysis of the material being used and should involve using thermal treatments to remove the grown-in defects [35]–[37]. In this regard, it would seem necessary to evaluate material from a range of manufacturers in order to minimize material lifetime discrepancies between various FZ manufacturers as the growth conditions of the FZ ingots vary amongst them.

2) p-type Silicon: Fig. 5(a) and (b) plot the injection-dependent effective lifetime of Al_2O_3 (purple squares) and SA (blue circles) treated p-type FZ-Si. Once again, it is clear from the figure that both schemes exhibit similar passivation levels; however, in this case, the injection dependence in the lifetime curves is not a result of surface recombination, but rather due to a bulk defect as evident by the extracted bulk lifetime from the etch-back experiments, where $\tau_{\rm bulk}$ declines monotonically for $\Delta n < 10^{15}$ cm^{-3}. In the case of Fig. 5(b), an accurate extraction of $\tau_{\rm bulk}$ could not be obtained for injection levels of $\Delta n < 10^{15}$ cm^{-3}, and therefore we have estimated the bulk lifetime (grey curve) by assuming a constant $J_{\rm os}$ of 2 ± 1 fA/cm^2 for the Al_2O_3 passivated 10 Ω·cm p-type sample ($J_{\rm os}$ of 2 ± 1 fA/cm^2 was determined for the Al_2O_3 passivated samples in this study) [43]. We note, aside from the lifetime-limiting defect in low injection, the high injection data agree well with the modeled intrinsic limit for both the 1 and 10 Ω·cm p-type samples.

From our etch-back re-passivation experiments on p-type silicon (not shown), we have extracted $\tau_{\rm bulk}$ of 3.5 ± 1.5 ms and a low S of 2.7 ± 1 cm/s (at $\Delta n = 10^{15}$ cm^{-3}) for 1 Ω·cm p-type silicon and $\tau_{\rm bulk}$ of 43 ± 10 ms and a very low S of 0.63 ± 0.07 cm/s (at $\Delta n = 10^{15}$ cm^{-3}) for 10 Ω·cm p-type silicon.

D. Surface Recombination Velocity Parameterization

Fig. 6(a) plots the doping dependence of S for SA-treated silicon wafers as determined from etch-back experiments shown in Figs. 4 and 5. The figure shows a monotonic increase in surface recombination with doping concentration, which can be approximated by a power regression of the form:

$$S_{\rm approx}\left(N_{\rm dop}\right) = a \cdot N_{\rm dop}^{b} \tag{2}$$

where $S_{\rm approx}$ is the approximated surface recombination velocity, $N_{\rm dop}$ is the doping concentration, and a and b are constants with values of $\exp(-20.2 \mp 3.15)$ cm^4/s and 0.57 ± 0.09, respectively.

Equation (2) is, therefore, a general parameterization for SA-treated silicon, provided the process flow outlined in Section II is followed carefully. Furthermore, the parameterization governed by (2) is only applicable for injection levels $< 10^{15}$ cm^{-3}, which results because the surface recombination converges to a constant value, while for high injection levels ($>10^{15}$ cm^{-3}), this is not necessarily true as demonstrated in Fig. 6(b). Fig. 6(b) plots the injection dependence of the surface recombination velocity for each material used in the parameterization. For 1 (green squares) and 10 Ω·cm (red diamonds), p-type silicon S remains relatively constant with injection level, thus implying the interface is governed by a low interface defect density (chemical passivation) rather than a field effect passivation mechanism resulting from charge in the film. In contrast, 1 Ω·cm n-type silicon (blue circles) does show injection dependence for $\Delta p > 10^{15}$ cm^{-3}; however, we postulate the decline in S with an increase in Δp is due to an error in the measurement of $\tau_{\rm bulk}$, where the bulk lifetime should be slightly higher than we have measured. Consequently, S should be higher when $\Delta p > 10^{15}$ cm^{-3}. Nevertheless, the error bars for 1 Ω·cm n-type silicon indicate S should be relatively constant over the injection level range investigated and thus also indicate the dominance of chemical passivation. The injection dependence observed for 10 Ω·cm n-type silicon, however, does indicate some level of charge (positive or negative) could be present in the film, evident by the rise in S with an increase in Δp (or Δn). Nevertheless, experimental results indicate chemical

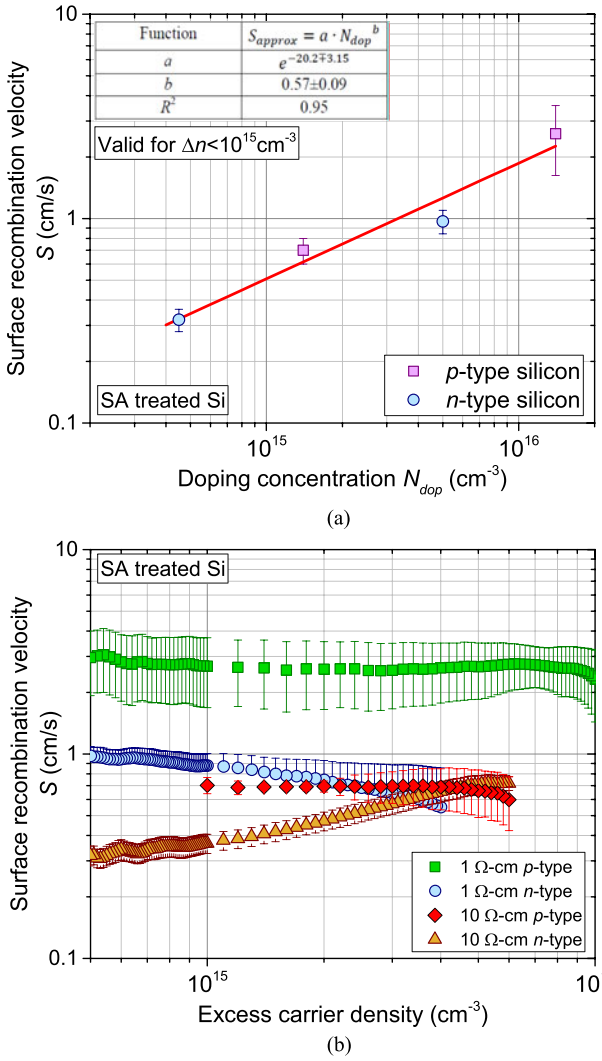

Fig. 6. (a) S versus doping concentration for SA-treated silicon wafers. The red line represents the best fit to the data (power regression), yielding an approximate surface recombination parameterization for SA-treated silicon, which is valid for injection levels $< 10^{15}$ cm^{-3}. (b) S versus excess carrier density for 1, 10 Ω·cm n- and p-type SA-treated silicon.

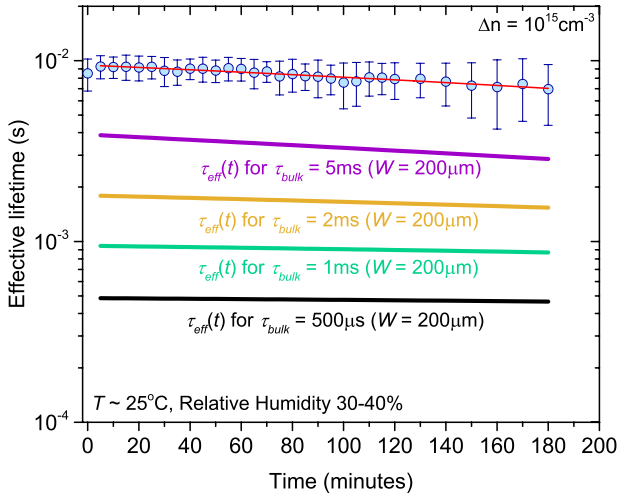

Fig. 7. Effective lifetime versus time (minutes) for an SA-treated 5 Ω·cm FZ n-type 750 μm silicon wafer (blue circles). The data are averaged over three separate experiments, where the red line is our best estimate of the degradation rate. The modeled degradation curves represent the case when the silicon wafer is thin (200 μm) with varying bulk lifetime values.

passivation is the predominant mechanism for SA-treated silicon, thereby validating the parameterization of Fig. 6(a), which otherwise would not hold for both n- and p-type silicon. In light of this finding, we postulate that the increase in S with doping concentration shown in Fig. 6(a) is primarily caused by a monotonic increase in the interface defect density (D_{it}) as S of uncharged (or very low charge) films should not exhibit doping dependence (for constant D_{it}) as justified in [43].

E. Prospects for Superacid-Treated Silicon: Applications for Materials Characterization

While a very high level of surface passivation has been demonstrated in this work, we note these films do experience degradation when exposed to ambient air conditions as demonstrated in Fig. 7.

Fig. 7 plots the degradation of an FZ 5 Ω·cm n-type sample over a 3 h period, where the error bars represent the standard deviation averaged over three separate experiments. The red line through the data (blue circles) corresponds to a linear regression, in which a degradation rate in S of 0.0052 cm/s/min [converting τ_{eff} to S using (1)] could be determined. If in contrast the bulk lifetime were lower (compared to the sample used), then the same degradation rate of 0.0052 cm/s/min would show less overall degradation in the measured lifetime over the 3 h period as modeled in Fig. 7. The modeled degradation curves were calculated using (1), where $W = 200\,\mu$m, $S = 0.0052 \cdot \mathrm{time(min)} + S_{\mathrm{approx}}(N_{\mathrm{dop}})$, and τ_{bulk} was sequentially varied from 500 μs to 5 ms as shown in Fig. 7. These modeled degradation curves, thus, represent cases in which material characterization is not time critical, i.e., when $\tau_{\mathrm{bulk}} < 5$ ms, which is suitable for most mono- and multi-Si samples as demonstrated for mono-Si in Fig. 8(a) and (b).

Fig. 8(a) plots the injection-dependent bulk lifetime of an FZ p-type silicon wafer which has been passivated by a stack of Al_2O_3 and a-SiN$_x$:H and then subject to a rapid thermal anneal at 800 °C and subsequently illuminated (0.1 W/cm^2) for 1–2 hours as outlined in [44]. Under these conditions, a significant reduction in lifetime is observed [compared to Fig. 5(a)]; however, it is difficult to ascertain whether this reduction in lifetime is a result of degradation in the dielectric stack or the activation of a bulk defect. By removing the dielectric stack and re-passivating the sample with our SA treatment, it is clear that the reduction in lifetime was due to the activation of a bulk defect, evident by the similarity in the measured lifetime curve for both passivation schemes. Through a Shockley–Read–Hall (SRH) analysis, defect parameters can be deduced from the measured lifetime curve as demonstrated in Fig. 8(a). To quantify the spatial distribution of the defect, the SA-treated sample in Fig. 8(a) was subject to PL imaging, which shows "ring-like" defect structures resulting from the growth conditions as seen in Fig. 8(b). In this case, the defect has been attributed to hydrogen complexes (from the dielectric stack) interacting with grown-in

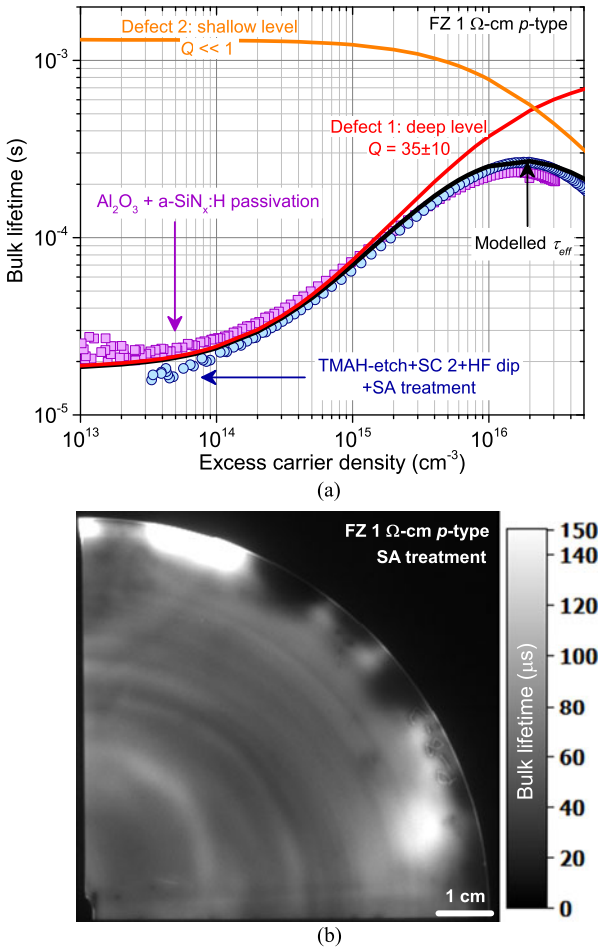

Fig. 8. (a) Injection-dependent bulk lifetime of dielectric passivated (purple squares) and SA-treated (blue circles) 1 Ω·cm FZ p-type silicon. The black solid line corresponds to the modeled lifetime based on an SRH analysis while the red (defect 1) and orange (defect 2) lines correspond to the individual defects which result in the shape of the measured lifetime curve. (b) PL image of the SA-treated sample measured in (a).

defects [44], which otherwise would have been difficult to determine without the SA treatment. We note, PL images are only quantitative if the passivation film is spatially uniform, which is the case for SA-treated silicon.

With the development of high-quality room temperature passivation schemes such as SA-treated silicon, low-temperature gettering and hydrogenation techniques can be developed [18]–[21], which otherwise would be difficult to measure, if, for example, these methods relied on SiN_x and Al_2O_3 passivation, which in themselves can introduce hydrogen or change bulk properties through annealing procedures to activate the surface passivation (i.e., 400 °C) [44]–[46]. In this regard, the SA treatment can provide valuable information regarding passivation quality of dielectric films and their impact on the bulk material. Finally, it has recently been demonstrated that SA-based passivation can be used in the diagnosis of bulk lifetime degradation in the development of interdigitated back contact solar cells [47], where it allows the true bulk lifetime to be measured after junction removal by reducing the influence of thermal or hydrogenation effects.

IV. Conclusion

We have demonstrated a very high level of surface passivation by controlling the ambient environment (glovebox) and developing a surface conditioning procedure prior to immersing silicon into a superacid-containing solution. We demonstrated that the SA treatment is not sensitive to the silicon surface roughness, rather it depends on the wet chemical procedure prior to the SA treatment, where SC 2 followed by a 2% HF dip yields the best surface condition.

We have parameterized the surface recombination achieved by the SA treatment, and demonstrate its dependence on the doping concentration of the silicon substrate can be parameterized with a power regression. Analysis of the injection-dependent lifetime and surface recombination curves has revealed the dominance of chemical passivation; however, a small amount of field effect passivation from charge in the films cannot be ruled out. In most cases, an astonishingly low surface recombination velocity of <1 cm/s was achieved on n- and p-type silicon substrates, and as a result, we have measured what we believe to be the highest lifetime ever reported in Cz-Si (65 ms). We have also demonstrated that the surface recombination velocity in FZ-Si is comparable with those used in the record lifetime studies in that material. The quality of our surface passivation enables the measurement of lifetimes up to and probably beyond the intrinsic limit, casting doubt over the currently accepted parameterization.

Immediate applications of the passivation scheme extend to measuring bulk carrier lifetimes and thus reducing material-related losses in silicon devices. The passivation scheme is expected to help elucidate mechanisms associated with low-temperature gettering and hydrogenation techniques, owing to the excellent passivation quality and low-temperature (<100 °C) deposition/processing conditions. While SA-based passivation schemes do exhibit degradation under ambient conditions, future applications may find such films in high-efficiency tandem devices, provided stability issues can be resolved, a common trait amongst organic thin film electronic materials. The exceptionally high level of surface passivation offered by SA-based films is expected to help extend the limits of surface and bulk lifetimes for PV applications.

Acknowledgment

The authors thank Dr. R. Falster for helpful discussions and Dr. J. Benick for organizing the thermal processing and ALD Al_2O_3 passivation of the silicon wafers used in this work. Data published in this paper can be freely downloaded from http://wrap.warwick.ac.uk/92115.

References

[1] O. Schultz, S. W. Glunz, and G. Willeke, "Multicrystalline silicon solar cells exceeding 20% efficiency," *Prog. Photovolt. Res. Appl.*, vol. 12, pp. 553–558, 2004.

[2] J. Haunschild, I. E. Reis, J. Geilker, and S. Rein, "Detecting efficiency-limiting defects in Czochralski-grown silicon wafers in solar cell production using photoluminescence imaging," *Phys. Status Solidi Rapid Res. Lett.*, vol. 5, pp. 199–201, 2011.

[3] J. D. Murphy, R. E. McGuire, K. Bothe, V. V. Voronkov, and R. J. Falster, "Minority carrier lifetime in silicon photovoltaics: The effect of oxygen precipitation," *Sol. Energy Mater. Sol. Cells*, vol. 120, pp. 402–411, 2014.

[4] Y. Wan, K. R. McIntosh, A. F. Thomson, and A. Cuevas, "Low surface recombination velocity by low-absorption silicon nitride on c-Si," *IEEE J. Photovolt.*, vol. 3, no. 1, pp. 544–559, Jan. 2013.

[5] A. Richter, S. W. Glunz, F. Werner, J. Schmidt, and A. Cuevas, "Improved quantitative description of Auger recombination in crystalline silicon," *Phys. Rev. B*, vol. 86, 2012, Art. no. 165202.

[6] S. Y. Herasimenka *et al.*, "Surface passivation of n-type c-Si wafers by a-Si/SiO_2/SiN_x stack with <1 cm/s effective surface recombination velocity," *Appl. Phys. Lett.*, vol. 103, 2013, Art. no. 183903.

[7] R. S. Bonilla, C. Reichel, M. Hermle, and P. R. Wilshaw, "Extremely low surface recombination in 1 Ω cm n-type monocrystalline silicon," *Phys. Status Solidi Rapid Res. Lett.*, vol. 11, 2017, Art. no. 1600307.

[8] K. Yoshikawa *et al.*, "Silicon heterojunction solar cell with interdigitated back contacts for a photoconversion efficiency over 26%," *Nature Energy*, vol. 2, 2017, Art. no. 17032.

[9] J. Werner *et al.*, "Efficient monolithic perovskite/silicon tandem solar cell with cell area >1 cm^2," *J. Phys. Chem. Lett.*, vol. 7, no. 1, pp. 161–166, 2016.

[10] Y. Xia, K. Sun, and J. Ouyang, "Solution-processed metallic conducting polymer films as transparent electrode of optoelectronic devices," *Adv. Mater.*, vol. 24, no. 18, pp. 2436–2440, 2012.

[11] Z. Yang *et al.*, "Tuning of the contact properties for high-efficiency Si/PEDOT:PSS heterojunction solar cells," *ACS Energy Lett.*, vol. 2, pp. 556–562, 2017.

[12] X. Zhang *et al.*, "Improved PEDOT:PSS/c-Si hybrid solar cell using inverted structure and effective passivation," *Sci. Rep.*, vol. 6, 2016, Art. no. 35091.

[13] J. Schmidt, V. Titova, and D. Zielke, "Organic-silicon heterojunction solar cells: Open-circuit voltage potential and stability," *Appl. Phys. Lett.*, vol. 103, 2013, Art. no. 183901.

[14] D. Zielke, A. Pazidis, F. Werner, and J. Schmidt, "Organic-silicon heterojunction solar cells on n-type silicon wafers: The BackPEDOT concept," *Sol. Energy Mater. Sol. Cells*, vol. 131, pp. 110–116, 2014.

[15] D. Zielke *et al.*, "Organic-silicon solar cells exceeding 20% efficiency," *Energy Procedia*, vol. 77, pp. 331–339, 2015.

[16] J. Chen *et al.*, "Silicon surface passivation by polystyrenesulfonate thin films," *Appl. Phys. Lett.*, vol. 110, 2017, Art. no. 083904.

[17] J. Bullock *et al.*, "Superacid passivation of crystalline silicon surfaces," *ACS Appl. Mater. Interfaces*, vol. 8, pp. 24205–24211, 2016.

[18] M. Al-Amin and J. D. Murphy, "Increasing minority carrier lifetime in as-grown multicrystalline silicon by low temperature internal gettering," *J. Appl. Phys.*, vol. 119, 2016, Art. no. 235704.

[19] M. Al-Amin and J. D. Murphy, "Passivation effects on low temperature gettering in multicrystalline silicon," *IEEE J. Photovolt.*, vol. 7, no. 1, pp. 68–77, Jan. 2017.

[20] A. Y. Liu *et al.*, "Gettering of interstitial iron in silicon by plasma-enhanced chemical vapour deposited silicon nitride films," *J. Appl. Phys.*, vol. 120, 2016, Art. no. 193103.

[21] P. Hamer *et al.*, "A novel source of atomic hydrogen for passivation of defects in silicon," *Phys. Status Solidi Rapid Res. Lett.*, vol. 11, no. 5, 2017, Art. no. 1600448.

[22] W. Kern, "The evolution of silicon wafer cleaning technology," *J. Electrochem. Soc.*, vol. 137, pp. 1887–1892, 1990.

[23] K. L. Luke and L.-J. Cheng, "A chemical/microwave technique for the measurement of bulk minority carrier lifetime in silicon wafers," *J. Electrochem. Soc.*, vol. 135, pp. 957–961, 1988.

[24] T. Trupke, R. A. Bardos, M. C. Schubert, and W. Warta, "Photoluminescence imaging of silicon wafers," *Appl. Phys. Lett.*, vol. 89, 2006, Art. no. 044107.

[25] A. L. Blum *et al.*, "Inter-laboratory study of eddy-current measurement of excess-carrier recombination lifetime," *IEEE J. Photovolt.*, vol. 4, no. 1, pp. 525–531, Jan. 2014.

[26] K. Yamamoto, A. Nakamura, and U. Hase, "Control of cleaning performance of an ammonia and hydrogen peroxide mixture (APM) on the basis of a kinetic reaction model," *IEEE Trans. Semicond. Manuf.*, vol. 12, no. 3, pp. 288–294, Aug. 1999.

[27] K. Hiroyuki, R. Jiro, S. Takayuki, and S. Yasushi, "Study of Si Etch rate in various composition of SC1 solution," *Jpn. J. Appl. Phys.*, vol. 32, no. 1A, 1993, Art. no. L45.

[28] M. Miyashita, T. Tusga, K. Makihara, and T. Ohmi, "Dependence of surface microroughness of CZ, FZ, and EPI wafers on wet chemical processing," *J. Electrochem. Soc.*, vol. 139, no. 8, pp. 2133–2142, 1992.

[29] W. Kern, *RCA Critical Cleaning Process*. Belmont, CA, USA: MicroTech Syst.,, 2007.

[30] T. Trupke *et al.*, "Effective excess carrier lifetimes exceeding 100 ms in float zone silicon determined from photoluminescence," in *Proc. 19th Eur. Photovolt. Sol. Energy Conf.*, 2004, pp. 758–761.

[31] E. Yablonovitch, D. L. Allara, C. C. Chang, T. Gmitter, and T. B. Bright, "Unusually low surface-recombination velocity on silicon and germanium surfaces," *Phys. Rev. Lett.*, vol. 57, pp. 249–252, 1986.

[32] N. E. Grant, K. R. McIntosh, and J. T. Tan, "Evaluation of the bulk lifetime of silicon wafers by immersion in hydrofluoric acid and illumination," *ECS J. Solid State Sci. Technol.*, vol. 1, pp. P55–P61, 2012.

[33] N. E. Grant, "Light enhanced hydrofluoric acid passivation: A sensitive technique for detecting bulk silicon defects," *J. Vis. Exp.*, vol. 107, 2016, Art. no. e53614.

[34] A. B. Sproul, "Dimensionless solution of the equation describing the effect of surface recombination on carrier decay in semiconductors," *J. Appl. Phys.*, vol. 76, no. 5, pp. 2851–2854, 1994.

[35] N. E. Grant *et al.*, "Thermal activation and deactivation of grown-in defects limiting the lifetime of float-zone silicon," *Phys. Status Solidi Rapid Res. Lett.*, vol. 10, pp. 443–447, 2016.

[36] N. E. Grant *et al.*, "Permanent annihilation of thermally activated defects which limit the lifetime of float-zone silicon," *Phys. Status Solidi A*, vol. 213, pp. 2844–2849, 2016.

[37] N. E. Grant, F. E. Rougieux, D. Macdonald, J. Bullock, and Y. Wan, "Grown-in defects limiting the bulk lifetime of p-type float-zone silicon wafers," *J. Appl. Phys.*, vol. 117, no. 5, 2015, Art. no. 055711.

[38] J. J. H. Gielis, B. Hoex, M. C. M. van de Sanden, and W. M. M. Kessels, "Negative charge and charging dynamics in Al_2O_3 films on Si characterized by second-harmonic generation," *J. Appl. Phys.*, vol. 104, no. 7, 2008, Art. no. 073701.

[39] T. Kho *et al.*, "Optimization and characterization of ONO," submitted for publication.

[40] T. Niewelt, W. Kwapil, M. Selinger, A. Richter, and M. C. Schubert, "Long-term stability of aluminum oxide based surface passivation schemes under illumination at elevated temperatures," *IEEE J. Photovolt.*, vol. 7, no. 5, pp. 1197–1202, Sep. 2017. doi: 10.1109/JPHOTOV.2017.2713411.

[41] M. J. Kerr and A. Cuevas, "General parameterization of Auger recombination in crystalline silicon," *J. Appl. Phys.*, vol. 91, pp. 2473–2480, 2002.

[42] J. Schmidt, M. Kerr, and P. P. Altermatt, "Coulomb-enhanced Auger recombination in crystalline silicon at intermediate and high injection densities," *J. Appl. Phys.*, vol. 88, no. 3, pp. 1494–1497, 2000.

[43] K. R. McIntosh and L. E. Black, "On effective surface recombination parameters," *J. Appl. Phys.*, vol. 116, 2014, Art. no. 014503.

[44] T. Niewelt *et al.*, "Light-induced activation and deactivation of bulk defects in boron-doped float-zone silicon," *J. Appl. Phys.*, vol. 121, no. 18, 2017, Art. no. 185702.

[45] F. E. Rougieux, N. E. Grant, C. Barugkin, D. Macdonald, and J. D. Murphy, "Influence of annealing and bulk hydrogenation on lifetime limiting defects in nitrogen-doped floating zone silicon," *IEEE J. Photovolt.*, vol. 5, no. 2, pp. 495–498, Mar. 2015.

[46] D. Sperber, A. Herguth, and G. Hahn, "A 3-state defect model for light-induced degradation in boron-doped float-zone silicon," *Phys. Status Solidi Rapid Res. Lett.*, vol. 11, 2017, Art. no. 1600408.

[47] T. Rahman *et al.*, "Minimising bulk lifetime degradation during the processing of interdigitated back contact silicon solar cells," *Prog. Photovolt. Res. Appl.*, 2017, published online, doi: 10.1002/pip.2928.

Authors' photographs and biographies not available at the time of publication.